

## **SURFACE-HARDENABLE HEAT TREATED P/M STEELS**

**W. Brian James and Robert J. Causton  
Hoeganaes Corporation  
Riverton, NJ 08077  
USA**

**Presented at the Powder Metallurgy World Congress,  
San Francisco, CA, June 21-26, 1992**

### **ABSTRACT**

The addition of fine particles ( $< 20\mu\text{m}$ ) of high-carbon ferroalloys to the high compressible prealloy powders, Ancorsteel® 85 HP and Ancorsteel 150 HP, has been shown to be a practical way of producing ferrous low-alloy steels containing chromium and manganese.

Increased sintering temperatures improved the mechanical properties of the materials and the effect was particularly noticeable at 2350°F.

The ferroalloy additions significantly enhanced the hardenability of the base low-alloys. Materials based on the low-alloy powder containing 1.5% molybdenum were more hardenable than those based on the 0.85% molybdenum alloy.

These materials are well suited for plasma nitriding and should find use in gears and cams that require a hard wear-resistant surface coupled with a strong, tough core.

### **INTRODUCTION**

Chromium and manganese are used extensively as alloy additions in wrought steels because they are efficient enhancers of hardenability and mechanical properties. A strong affinity for oxygen has restricted their use in ferrous P/M low-alloys and powder metallurgists have developed low-alloy powders with nickel, copper, and molybdenum as the primary alloying additions. The latter form oxides during the water atomization process that can be reduced during the annealing stage of powder production, whereas chromium and manganese form extremely stable oxides that are not reducible under standard powder annealing conditions. The Ellingham diagram (Figure 1) provides a guide to the equilibrium thermodynamic factors associated with oxide reduction (1). In practice, reaction kinetics also play an important role.

The equilibrium conditions for metal oxides and metals in a pure hydrogen atmosphere are shown in Figure 2(2,3). The oxides of nickel, copper, and molybdenum are readily reduced in a high dew point atmosphere at conventional sintering temperatures ( $2100^{\circ}\text{F}$

or 1150°C). However, a dew point below minus 58°F (minus 50°C) is required to reduce the oxides of chromium and manganese at these sintering temperatures and this is well below the range of conventional atmosphere sintering furnaces. If alloy additions are present as oxides they do not contribute to the hardenability or strength of the alloy.

A number of approaches have been used to develop ferrous low-alloys containing chromium and manganese (4-12):

- Water atomization and vacuum annealing
- Oil atomization
- Masteralloys (MCM)
- Ferroalloy additions

In the water atomization plus vacuum reduction process, developed by Kawasaki Steel (7), a controlled amount of carbon contained in water atomized steel powder reduces oxides during annealing in vacuum. Parts produced from powders made by this method are still, however, susceptible to oxidation during sintering.

Oil atomization results in lower as-atomized oxygen contents for chrome/manganese containing low-alloy steel powders than are possible with water atomization (8). However, the powders need to be annealed to reduce their carbon content and considerable care must be taken during annealing to balance the conflicting requirement to maintain a low oxygen content as well as reduce the carbon level (5).

In the masteralloy approach, master alloys based on complex carbides are added to a high compressibility iron powder base (9,10). The MCM alloy contains 20% Mn, 20% Cr, 20% Mo, and 7% C. Zapf, Hoftmann, and Dalal successfully developed suitable masteralloys but the technique has not found widespread acceptance.

Tengzelius has presented the results of experiments using additions of finely ground low-carbon ferroalloys of chromium and manganese to iron powders (11,12). The chemical activity of chromium and manganese is reduced when they are introduced as ferroalloys rather than as elemental additions. The materials investigated had chromium and manganese contents of between 1 and 2%. The resulting samples had good mechanical properties when sintered at 2282°F (1250°C) but dimensional change was found to be particularly sensitive to carbon content and these materials have also failed to achieve widespread acceptance.

In the experimental work summarized below, chromium and manganese were added as finely ground high-carbon ferroalloys. The ferroalloy additions were made to highly compressible, water

atomized low-alloy powders with prealloyed molybdenum as their principal alloying addition. These recently developed low-alloy powders have compressibilities similar to those of plain iron powders (13, 14). The prealloyed molybdenum increases the yield strength of the resulting materials and makes a significant contribution to hardenability. The binder treatments currently used for premixes (15, 16) were not available when Tengzelius experimented with ferroalloy additions. These recently developed binder treatments permit the use of finer ferroalloy particle sizes in premixes, and minimize their tendency for segregation and dusting during subsequent processing (17).

## **EXPERIMENTAL PROCEDURE**

### **Materials**

The highly compressible, water atomized, prealloyed powder, Ancorsteel 85 HP was used as a base for the materials investigated. Ancorsteel 150 HP was also used as a base in selected trials in order to evaluate the effect of 1.5% compared with 0.85% prealloyed molybdenum. The typical chemical composition of these powders is presented in Table 1 and their compressibility and green strength characteristics are summarized in Figures 3 and 4. High-carbon ferroalloys of chromium and manganese were ground to 90% less than 20 micrometers and added to each of the base powders in the appropriate quantities to result in the chromium and manganese contents shown in the experimental matrix of Table 2. The ferroalloys contained about 6% carbon and approximately 70% of either chromium or manganese. Particle size characteristics of the ground ferroalloys are presented in Table 3. A 0.4% addition of Asbury 3203 natural flake graphite was made to each premix along with 0.5% Witco Lubrazinc-W zinc stearate (except where otherwise indicated).

The experimental matrix was subsequently repeated with an addition of 1% Inco 123 nickel powder to offset the growth from die size experienced with the initial samples.

### **Test Specimen Preparation**

Transverse rupture bars (TRS bars) were compacted in accordance with ASTM B 528 and flat, unmachined "dog-bone" tensile bars were made to the dimensions specified in ASTM E 8. The test bars were compacted at 45 tsi and sintered using a pusher furnace and a dissociated ammonia atmosphere with a dew point of between minus 4 to minus 10°F. Sintering temperatures of 2050°F, 2150°F, 2250°F, and 2350°F were used and samples were maintained at the sintering temperature for 30 minutes before being pushed into the water jacketed cooling zone of the furnace. (The sintering temperature of 2150°F was omitted for the samples with 1%

nickel).

In addition to being tested in the "as-sintered" condition, tensile specimens were austenitized at 1600°F for 1 hour in a dissociated ammonia atmosphere with methane added to maintain an appropriate carbon potential. The samples were quenched into oil preheated to 150°F. Tempering was performed for 1 hour in a nitrogen atmosphere. Tempering temperatures from 300°F to 1040°F were investigated.

### **Plasma Nitriding**

The TRS and tensile bars that were sintered at 2350°F for 30 minutes in a dissociated ammonia atmosphere were subsequently austenitized at 1650°F for 1 hour. These samples were quenched into oil preheated to 150°F. Tempering was performed for 1 hour at 950°F in a nitrogen atmosphere. The quench-hardened test bars were then plasma nitrided by Metal Plasma Technology America Corporation at their California Service Center.

### **Mechanical Property Testing**

Tensile testing was performed on an Instron tester at a crosshead speed of 0.1 inches/minute in accordance with ASTM E 8. The percentage dimensional change of the materials with respect to die size was measured on TRS bars following ASTM B 610 guidelines.

### **Jominy Hardenability**

Jominy hardenability test bars were machined from 4 inch diameter, 1.25 inch high powder forged compacts of selected materials. Hardenability testing was performed in accordance with ASTM A 255. The Jominy hardenability bars were austenitized at 1600°F for 30 minutes prior to quenching.

### **Metallographic Examination**

Sample cross-sections were cut from selected test specimens and prepared for metallographic examination. All metallographic preparation was done on a Struers Abrapol automated grinder/polisher following previously reviewed procedures (18).

## **RESULTS**

### **Mechanical Properties**

Tensile strength data for the "as-sintered" materials are summarized in Tables 4 through 10. These tables also include information on percentage dimensional change and apparent

hardness of the samples. The affect of sintering temperature is illustrated graphically for selected materials in Figures 5-7.

Tempering curves for quench-hardened tensile specimens containing 1% nickel, 0.75% chromium, and 0.75% manganese are presented in Figure 8 (Table 11) and show the affect of the higher prealloyed molybdenum content in the Ancorsteel 150 HP.

### **Jominy Hardenability**

Jominy hardenability curves for selected materials are presented in Figures 9 and 10 which highlight the effect of the various alloy additions and the influence of the base low-alloy powder on hardenability.

### **Metallography**

Photomicrographs of selected "as-sintered", and quench-hardened and plasma nitrided materials are shown in Figures 11-13.

## **DISCUSSION**

### **"As-Sintered" Materials**

The tensile strength of all of the "as-sintered" materials improved with increased sintering temperature (Tables 4-10 and Figures 5-7). The effect was particularly noticeable for the samples containing chromium and those with higher levels of manganese when sintered at 2350°F. A photomicrograph of the sample based on the 0.85% molybdenum prealloy with 1% nickel, 0.75% chromium, and 0.75% manganese, sintered at 2350°F is shown in Figure 11. The microstructure consists of a uniform dispersion of divorced pearlite. The reduced growth that results from the presence of the 1% nickel in this material is shown in Figure 14.

The effect of compaction pressure was investigated for selected materials based on both the 0.85% and the 1.5% molybdenum containing prealloys. Tensile properties for samples sintered at 2350°F are summarized in Figures 15 and 16. For compaction pressures of 40 tsi and above, the beneficial effect of both chromium and manganese can be seen. Little difference is observed between the tensile properties of materials made from the two base powders.

Graphite additions of 0.2% and 0.4% were evaluated for samples, based on both of the prealloyed powders, to which 1% nickel, 0.75% chromium, and 0.75% manganese had been added. These samples were compacted at 30, 40, and 50 tsi and sintered at 2350°F in dissociated ammonia. Good tensile properties were obtained even at the lower level of graphite addition (Figures 17 and 18). No

significant difference was observed between the tensile properties of materials made from the two low-alloy powders (Figure 19).

### **Quench-Hardened and Tempered Materials**

The tempering response of tensile samples containing 1% nickel, 0.75% chromium, and 0.75% manganese is shown in Figure 8. Samples based on the prealloy with 1.5% molybdenum retain their strength and hardness at higher tempering temperatures compared with those based on the prealloy containing 0.85% molybdenum.

### **Jominy Hardenability**

The beneficial effect of the added ferroalloys on hardenability is illustrated in Figures 9 and 10. The greater hardenability of the samples based on the prealloy with 1.5% molybdenum is apparent. Materials with both chromium and manganese had particularly good hardenability. The uniform microstructures shown in Figures 11-13 and the contribution to strength and hardenability resulting from the ferroalloy additions indicate the viability of the ferroalloy approach to producing ferrous low-alloys containing chromium and manganese.

### **Plasma Nitriding**

Plasma nitriding provides the ability to control compound layer thickness, maintain initial core hardness, and results in less distortion than gas nitriding because it can be performed at lower temperatures. A microhardness profile of the surface region of the sample based on the prealloy with 0.85% molybdenum is shown in Figure 20. This sample contained 1% nickel, 0.75% chromium, and 0.75% manganese along with an addition of 0.4% graphite. A photomicrograph of the core region of this sample is shown in Figure 12 and the surface region is illustrated in Figure 13.

### **CONCLUSIONS**

The addition of fine particles ( $< 20\mu\text{m}$ ) of high-carbon ferroalloys to highly compressible prealloyed powders is a practical way to produce ferrous low-alloys containing chromium and manganese.

The mechanical properties of the materials improved with increased sintering temperature and the effect was particularly noticeable at 2350°F.

The ferroalloy additions significantly enhanced the hardenability of the base low-alloys. Some of the resulting materials are

suitable for parts requiring heat treatment that have ruling sections of greater than 1.5 inches.

Materials based on the low-alloy powder containing 1.5% molybdenum were more hardenable than those based on the 0.85% molybdenum alloy.

These materials are well suited for plasma nitriding and should find use in gears and cams that require a hard wear-resistant surface coupled with a strong, tough core.

#### **ACKNOWLEDGMENTS**

The authors would like to acknowledge the contribution of J. D. Maguire to the early phases of this project. They are particularly grateful for the cooperation of the following personnel at Hoeganaes: R. Fitzpatrick, C. Gamble, T. Cimino, G. Golin, S. Kolwicz, and T. Murphy. The valuable discussions on plasma nitriding with A. B. Kassir and Joe Guerm of Metal Plasma Technology are also gratefully acknowledged.

#### **REFERENCES**

1. J. J. Dunkley, "Liquid Atomisation," Powder Metallurgy, Vol. 32, 1989, p. 96.
2. R. M. German, "Powder Metallurgy Science," 1964, p. 190, published by MPIF, Princeton, NJ.
3. A. Lawley, "Physicochemical Considerations in Powder Metallurgy," JOM, Vol. 42, No. 4, April 1990, p.12.
4. W. D. Jones, "Fundamental Principles of Powder Metallurgy," 1960, p. 568, published by Edward Arnold Ltd., London.
5. 5. Takajo, "Innovations in Ferrous Powders and their Production," published in Powder Metallurgy 1966-State of the Art, p. 11, Verlag Schmid GmbH, Freiburg, Germany.
6. F. J. Hanejko, "Mechanical Properties of Powder Forged 4100 and 1500 Type Alloy Steels," Modern Developments in Powder Metallurgy, Vol. 12, 1961, p. 689, published by MPIF, Princeton, NJ.
7. K. Ogura, R. Okabe, S. Takajo, N. Yamato, and Y. Maeda, "Production and Properties of Chromium-Containing Low-Oxygen Steel Powders," Progress in Powder Metallurgy, Vol. 43, 1987, p. 619, published by MPIF, Princeton, NJ.
8. E. Tamura and I. Karasuno, "Properties of Oil Atomized 4100

Low Alloy steel Powder," Progress in Powder Metallurgy, Vol. 41, 1965, p. 13, published by MPIF, Princeton, NJ.

9. G. Zapf, G. Hoffmann, and K. Dalal, "Effect of Additional Alloying Elements on the Properties of Sintered Manganese Steels," Powder Metallurgy, Vol. 18, No. 35, 1975, p. 214.

10. S. Banerlee, G. Schlieper, F. Thummler, and G. Zapf, "New Results in the Master Alloy Concept for High strength steels," Modern Developments in Powder Metallurgy, Vol. 13, 1961, p. 143, published by MPIF, Princeton, NJ.

11. J. Tengzelius and C-A. Blände, "High Temperature Sintering of P/M Steels," Powder Metallurgy International, Vol. 16, No. 3, 1964, p. 133.

12. J. Tengzelius, S-E. Grek, and C-A. Blände, "Limitations and Possibilities in the Utilization of Cr and Mn as Alloying Elements in High strength Sintered Steels," Modern Developments in Powder Metallurgy, Vol. 13, 1961, p. 159, published by MPIF, Princeton, NJ.

13. J. J. Fulmer and R. J. Causton, "Tensile, Impact and Fatigue Performance of a New Water Atomized Low-Alloy Powder-Ancorsteel 85 HP," Advances in Powder Metallurgy, 1990, Vol. 2, p. 459, published by MPIF, Princeton, NJ.

14. W. B. James, "High Performance Ferrous P/M Materials for Automotive Applications," Metal Powder Report, Vol. 46, No. 9, 1991, p. 26.

15. U.S. Patent No.4,483,905.

16. U.S. Patent No.4,834,800.

17. M. J. McDermott, "P/M Parts Fabrication Experience with ANCORBOND® (Binder Treated) Premixes, Advances in Powder Metallurgy, 1990, Vol. 1, p. 209, published by MPIF, Princeton, NJ.

18. R. J. Causton, T. F. Murphy, C-A. Blände, and H. Söderhjelm, "Nonmetallic Inclusion Measurement of Powder Forged Steels Using an Automatic Image Analysis System," Horizons of Powder Metallurgy 1966, Part II, p.727, published by Verlag Schmid GmbH, Freiburg, Germany.

**Table 1: Chemical composition of the base powders**

Composition (Weight %)				
Material	C	Mn	Mo	O



Ancorsteel 85 HP	<0.01	0.14	0.85	0.07
Ancorsteel 150 HP	<0.01	0.14	1.5	0.07

**Table 2: Experimental Matrix**  
Chromium and manganese additions made to Ancorsteel 85HP and Ancorsteel 150HP

Cr	Mn		
	0	0.75	1.5
0	X	X	X
0.75	X	X	
1.5	X		

**Table 3: Ferroalloy particle size (Microtrac analysis)**

% Passing	FeCr ( $\mu\text{m}$ )	FeMn ( $\mu\text{m}$ )
90	26.3	22.0
50	8.3	7.4
10	2.5	2.1

**Table 4: "As-sintered" properties - 0.85% Mo steel (0.4% gr.)**  
Test bars compacted at 45 tsi - sintered at 2050°F in DA

Material	Sintered Density ( $\text{g}/\text{cm}^3$ )	Yield psi ( $\times 10^3$ )	UTS psi ( $\times 10^3$ )	Elong. % (in 1 inch)	D.C. (%)	Apparent Hardness (HRB)
0.75% Cr	7.06	46.4	56.4	1.2	+0.25	79
1.5% Cr	7.01	48.5	64.1	1.2	+0.38	85
0.75% Mn	7.08	47.7	63.2	2.0	+0.17	78
1.5% Mn	7.04	53.1	71.8	1.9	+0.32	84
0.75% Cr + 0.75% Mn	7.02	54.4	71.9	1.8	+0.37	84

**Table 5: "As-sintered" properties - 0.85% Mo steel (0.4% gr.)**  
Test bars compacted at 45 tsi - sintered at 2150°F in DA

Material	Sintered Density ( $\text{g}/\text{cm}^3$ )	Yield psi ( $\times 10^3$ )	UTS psi ( $\times 10^3$ )	Elong. % (in 1 inch)	D.C. (%)	Apparent Hardness (HRB)
0.75% Cr	7.05	46.4	61.8	1.5	+0.28	80
1.5% Cr	7.00	54.8	76.5	1.6	+0.42	86

0.75% Mn	7.09	51.0	65.3	2.5	+0.14	77
1.5% Mn	7.03	55.3	73.9	2.4	+0.31	83
0.75% Cr + 0.75% Mn	7.02	56.6	78.9	2.0	+0.38	85

**Table 6: "As-sintered" properties - 0.85% Mo steel (0.4% gr.)  
Test bars compacted at 45 tsi - sintered at 2250°F in DA**

Material	Sintered Density (g/cm <sup>3</sup> )	Yield psi (x10 <sup>3</sup> )	UTS psi (x10 <sup>3</sup> )	Elong. % (in 1 inch)	D.C. (%)	Apparent Hardness (HRB)
0.75% Cr	7.06	49.7	67.8	2.1	+0.26	82
1.5% Cr	6.99	57.0	81.4	1.8	+0.48	87
0.75% Mn	7.10	51.1	66.2	2.9	+0.10	78
1.5% Mn	7.05	52.9	75.4	2.3	+0.28	83
0.75% Cr + 0.75% Mn	7.03	59.6	79.9	2.3	+0.34	86

**Table 7: "As-sintered" properties - 0.85% Mo steel (0.4% gr.)  
Test bars compacted at 45 tsi - sintered at 2350°F in DA**

Material	Sintered Density (g/cm <sup>3</sup> )	Yield psi (x10 <sup>3</sup> )	UTS psi (x10 <sup>3</sup> )	Elong. % (in 1 inch)	D.C. (%)	Apparent Hardness (HRB)
0.75% Cr	7.08	64.8	79.8	2.3	+0.29	81
1.5% Cr	7.01	78.9	97.9	1.8	+0.49	89
0.75% Mn	7.11	58.6	74.7	2.8	+0.11	79
1.5% Mn	7.06	72.6	89.5	2.0	+0.30	86
0.75% Cr + 0.75% Mn	7.03	73.5	92.8	2.0	+0.39	87

**Table 8: "As-sintered" properties - 0.85% Mo steel (1% Ni + 0.4% gr.) Test bars compacted at 45 tsi - sintered at 2050°F in DA**

Material	Sintered Density (g/cm <sup>3</sup> )	Yield psi (x10 <sup>3</sup> )	UTS psi (x10 <sup>3</sup> )	Elong. % (in 1 inch)	D.C. (%)	Apparent Hardness (HRB)
0.75% Cr	7.07	58.1	67.0	1.5	+0.20	84
1.5% Cr	7.00	65.7	76.6	1.5	+0.37	90
0.75% Mn	7.08	61.0	72.1	1.7	+0.15	84
1.5% Mn	7.03	74.6	87.7	1.7	+0.33	92

0.75% Cr + 0.75% Mn	7.02	69.6	83.8	1.8	+0.34	90
---------------------------	------	------	------	-----	-------	----

**Table 9: "As-sintered" properties - 0.85% Mo steel (1% Ni + 0.4% gr.) Test bars compacted at 45 tsi - sintered at 2250°F in DA**

Material	Sintered Density (g/cm <sup>3</sup> )	Yield psi (x10 <sup>3</sup> )	UTS psi (x10 <sup>3</sup> )	Elong. % (in 1 inch)	D.C. (%)	Apparent Hardness (HRB)
0.75% Cr	7.08	65.3	80.5	2.3	+0.11	86
1.5% Cr	7.00	80.3	100.1	1.7	+0.35	95
0.75% Mn	7.11	63.3	75.8	2.5	+0.13	83
1.5% Mn	7.04	75.1	90.2	2.2	+0.23	89
0.75% Cr + 0.75% Mn	7.02	77.3	93.6	2.1	+0.27	90

**Table 10: "As-sintered" properties - 0.85% Mo steel (1% Ni + 0.4% gr.) Test bars compacted at 45 tsi - sintered at 2350°F in DA**

Material	Sintered Density (g/cm <sup>3</sup> )	Yield psi (x10 <sup>3</sup> )	UTS psi (x10 <sup>3</sup> )	Elong. % (in 1 inch)	D.C. (%)	Apparent Hardness (HRB)
0.75% Cr	7.12	70.1	88.7	2.4	+0.13	86
1.5% Cr	7.04	89.8	113.8	1.5	+0.37	96
0.75% Mn	7.12	61.6	76.2	2.4	+0.12	81
1.5% Mn	7.06	81.2	103.8	1.8	+0.32	93
0.75% Cr + 0.75% Mn	7.05	86.5	106.7	1.6	+0.33	92

**Table 11: Tempering response of quench-hardened samples**

Material	Ultimate Tensile Strength (psi x 10 <sup>3</sup> )				
	Tempering Temperature (°F)				
		302	572	842	1040
0.75 Cr + 0.75% Mn (0.4% gr.)	0.85% Mo	94.6	139.4	131.9	129.0
	1.5% Mo	98.7	108.2	104.2	103.9
0.75% Cr + 0.75% Mn +	0.85% Mo	135.3	139.9	128.5	125.3
	1.5% Mo	118.8	138.9	135.6	138.8

1% Ni (0.4% gr.)				
---------------------	--	--	--	--

Material	Apparent Hardness (HRC)				
	Tempering Temperature (°F)				
		302	572	842	1040
0.75 Cr + 0.75 Mn (0.4% gr.)	0.85% Mo	45	33	32	27
	1.5% Mo	46	34	33	33
0.75% Cr + 0.75% Mn + 1% Ni (0.4% gr.)	0.85% Mo	44	32	32	28
	1.5% Mo	46	35	33	35

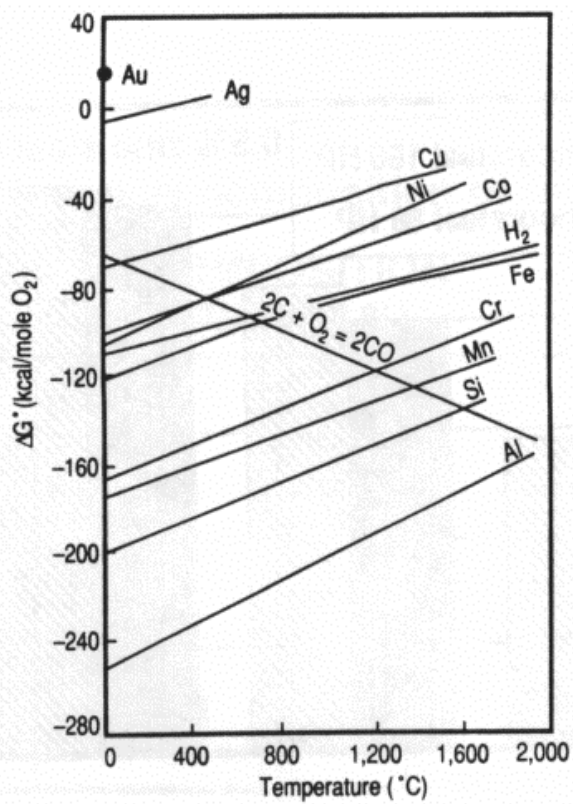


Figure 1: Ellingham diagram (reference 1).

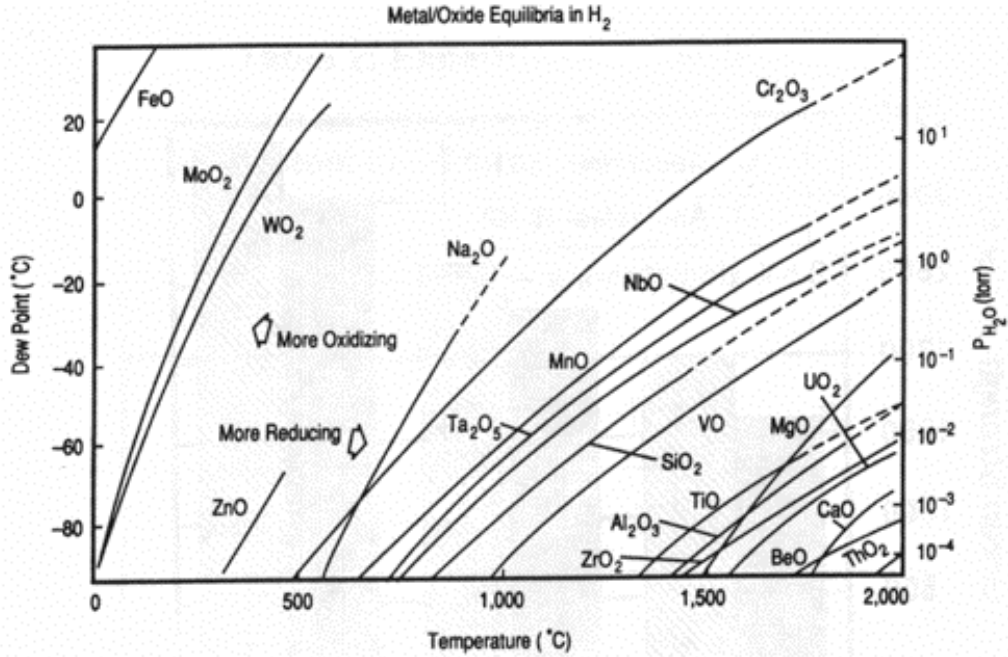


Figure 2: Equilibrium conditions for metals and metal oxides in a pure reducing atmosphere (H<sub>2</sub>) in terms of temperature and atmosphere dew point (2,3). Metals which are more easily reduced than those shown include copper and nickel.

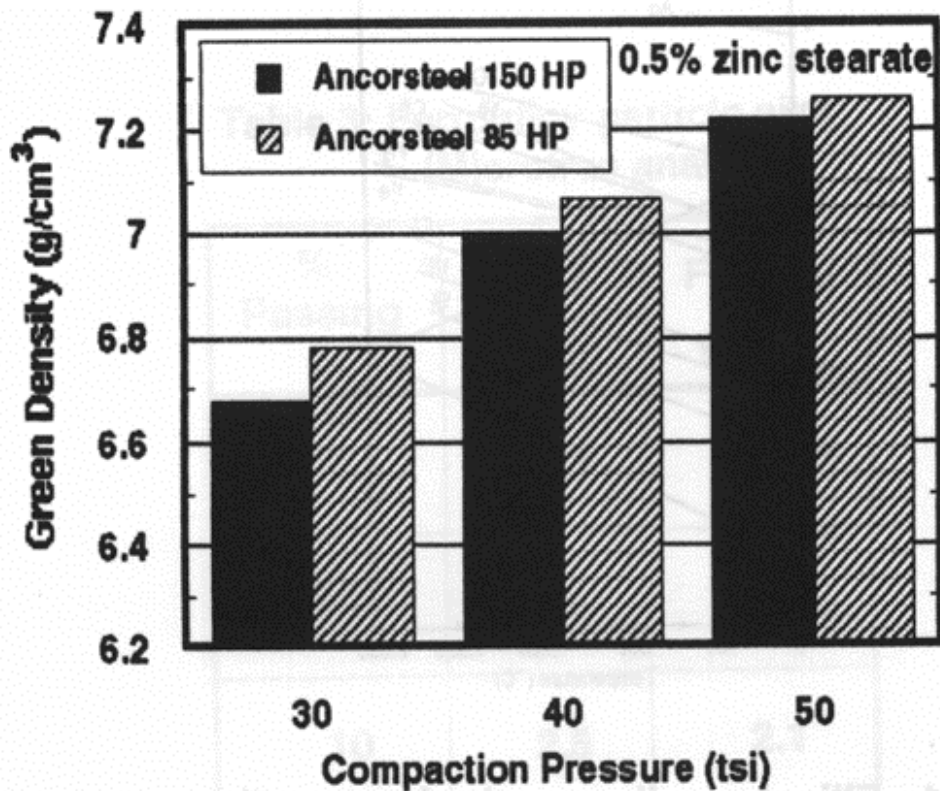


Figure 3: Compressibility of the low-alloy powders.

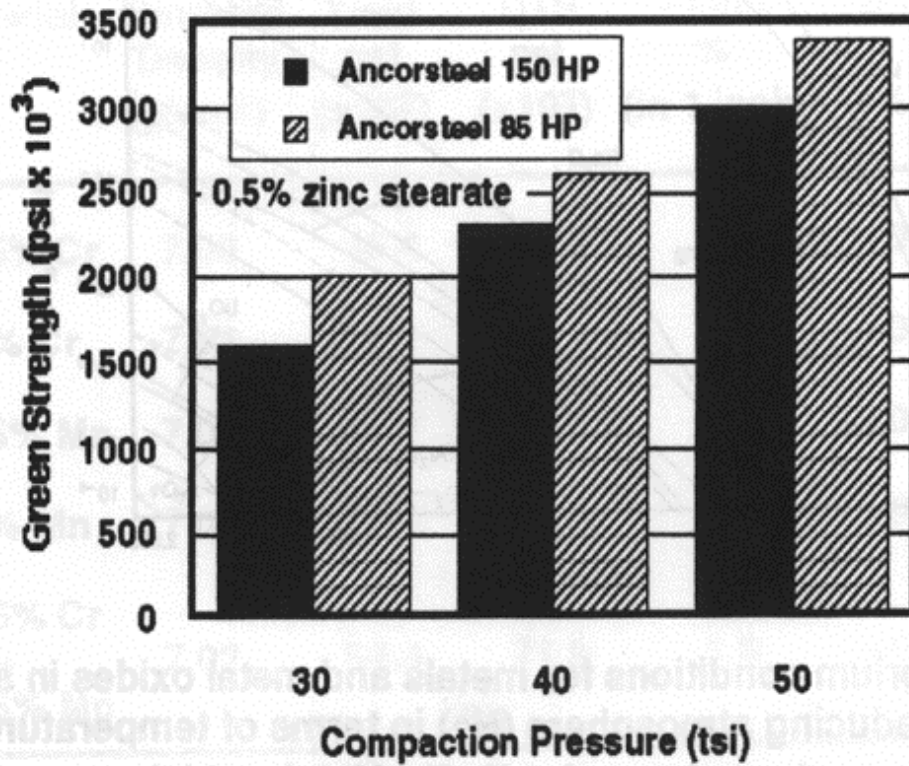


Figure 4: Green strength of the low-alloy powders.

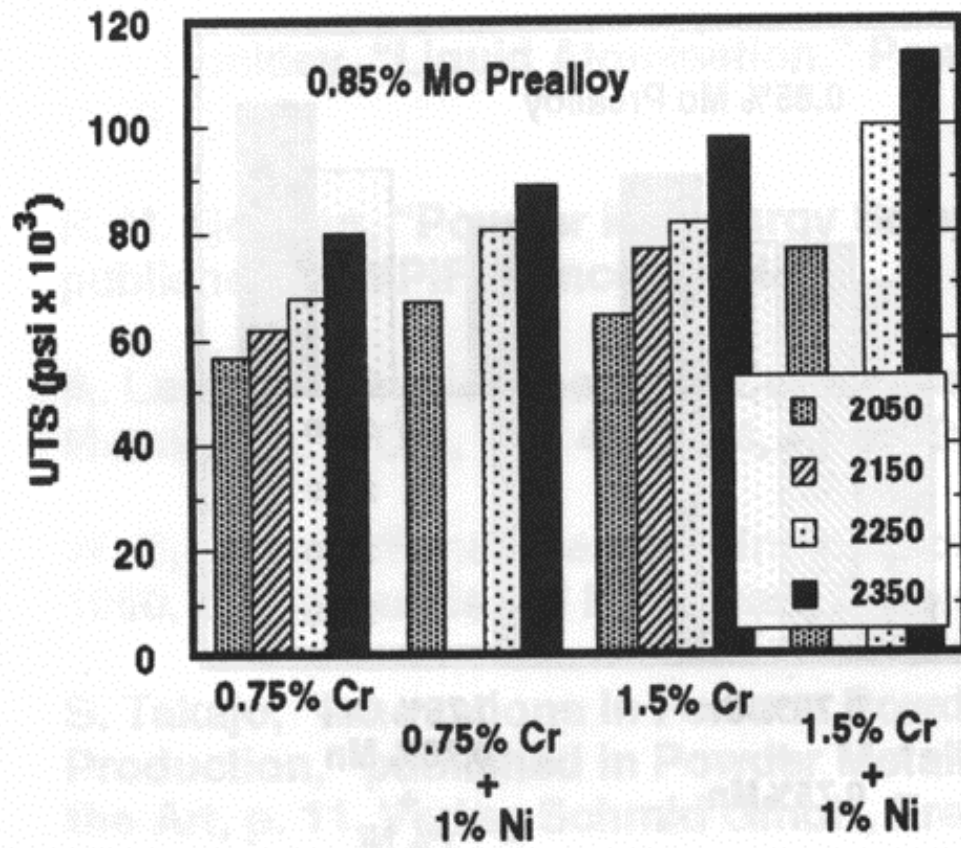


Figure 5: Effect of sintering temperature on UTS (45 tsi).

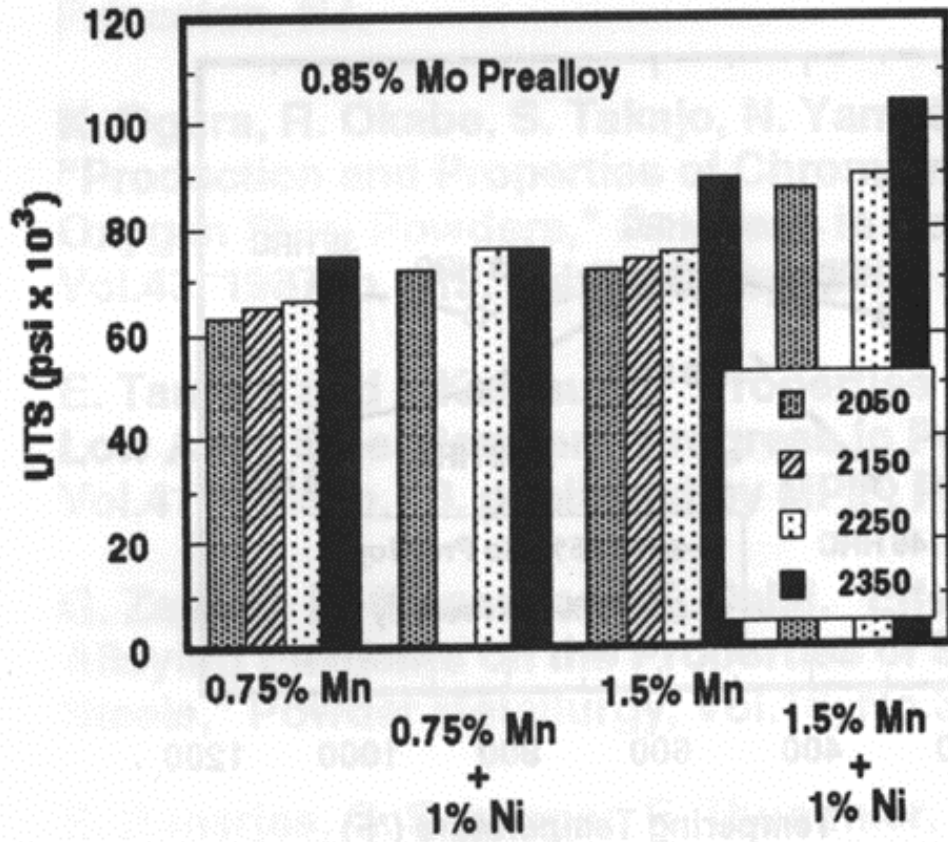


Figure 6: Effect of sintering temperature on UTS (45 tsi).



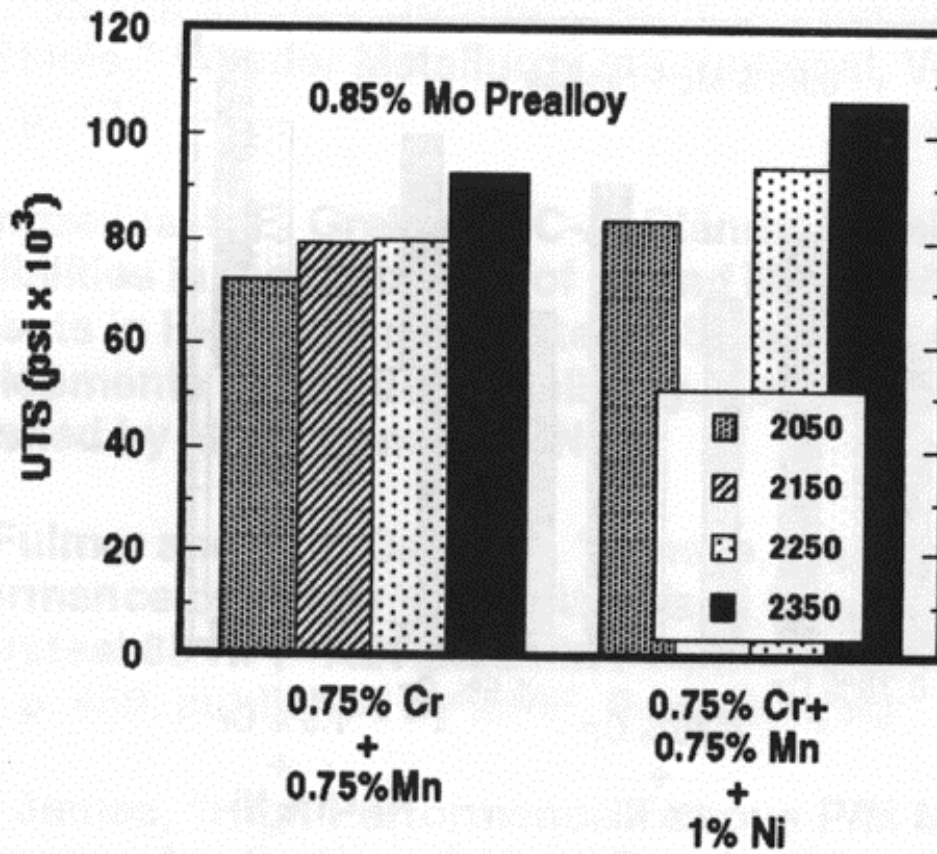


Figure 7: Effect of sintering temperature on UTS (45 tsi).

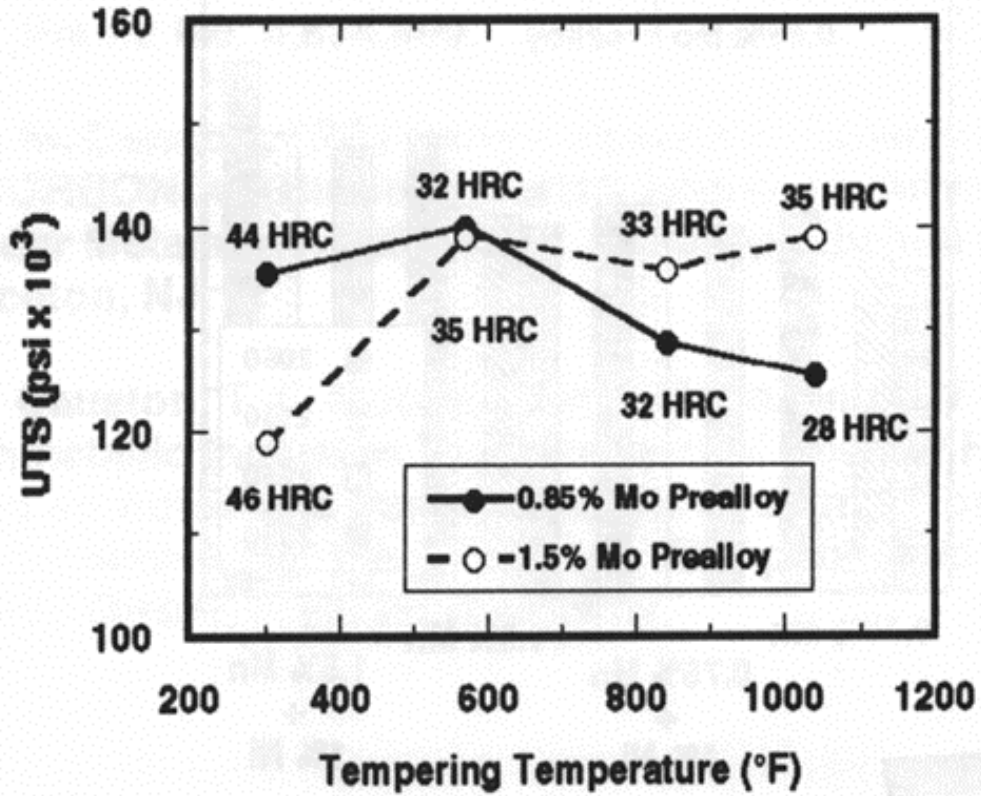


Figure 8: Effect of sintering temperature on UTS and apparent hardness (45 tsi).

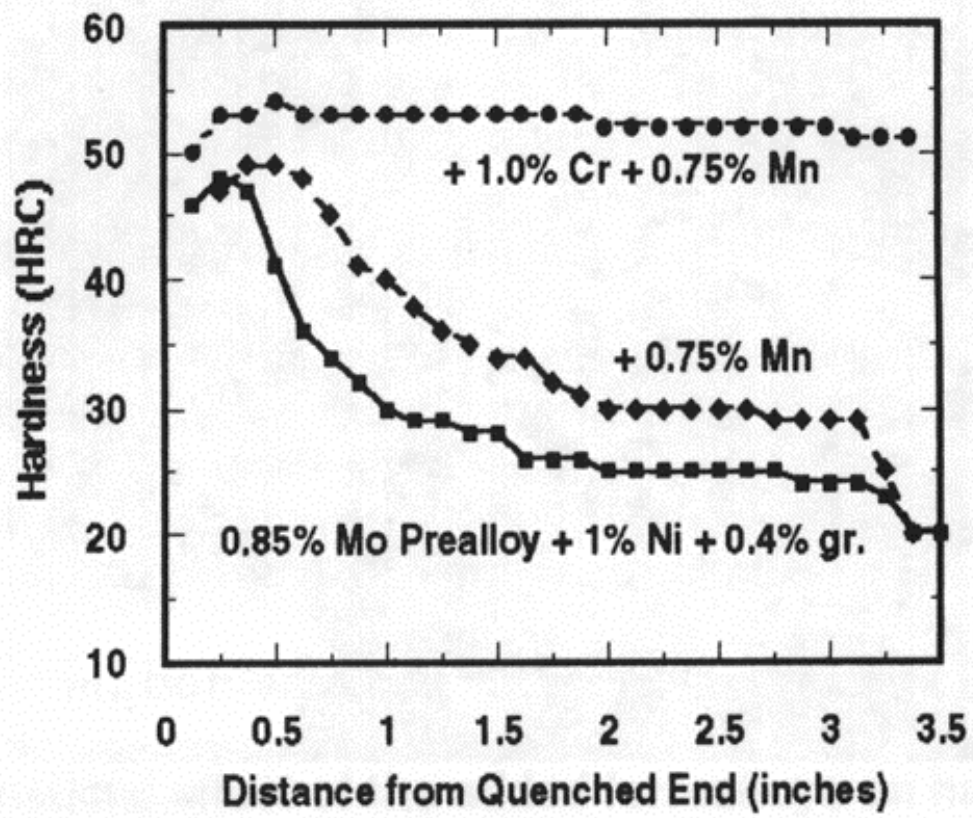


Figure 9: Jominy hardenability curves.

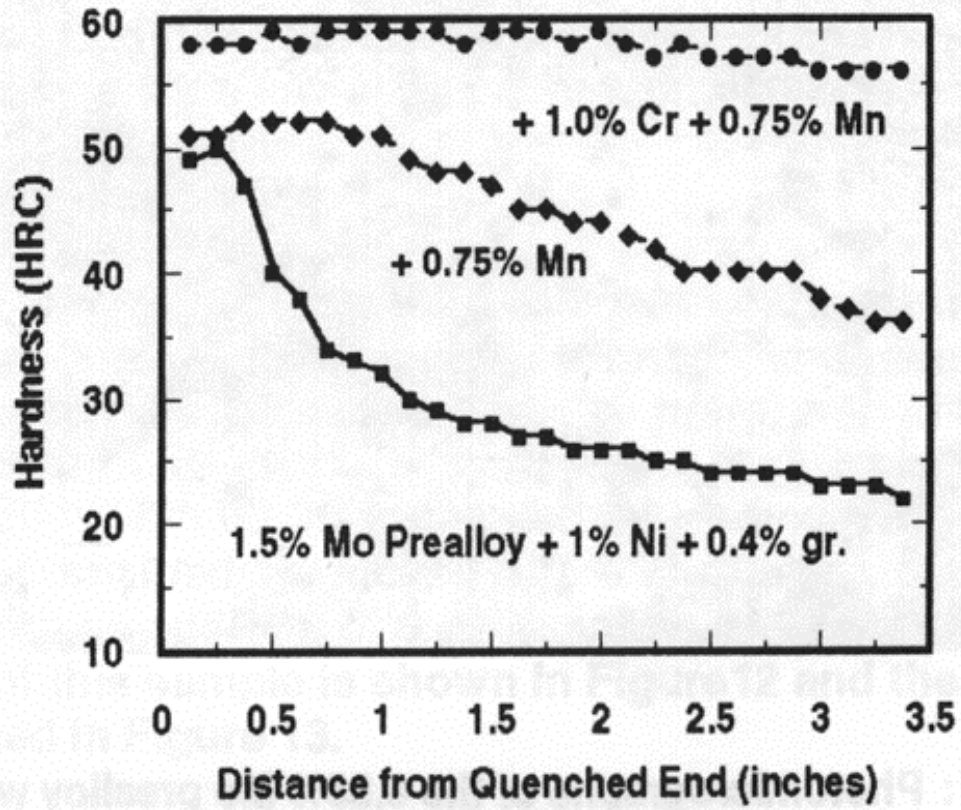
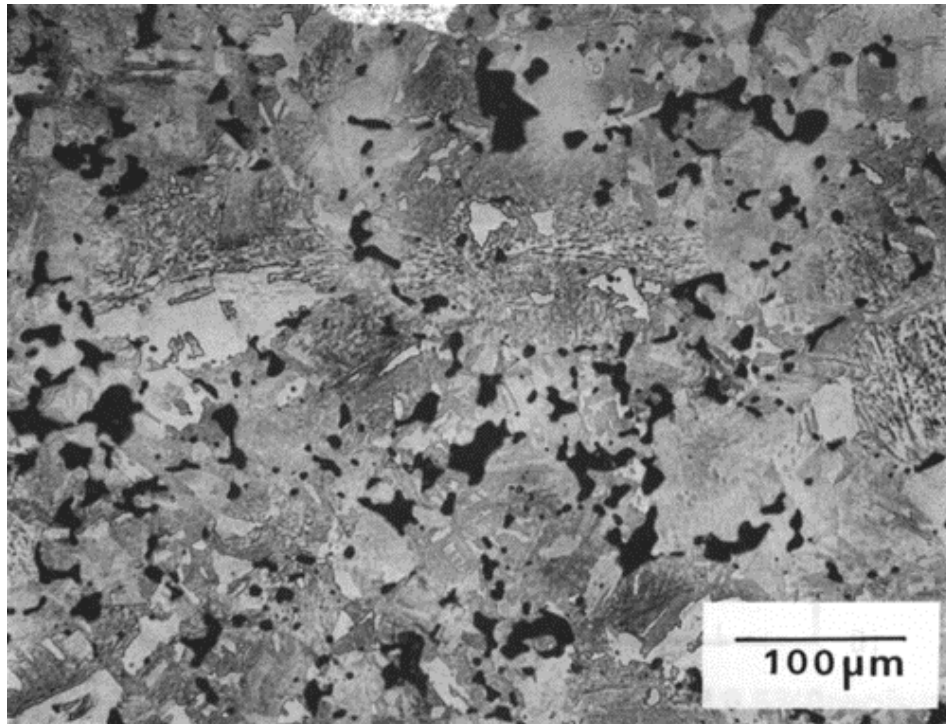


Figure 10: Jominy hardenability curves.



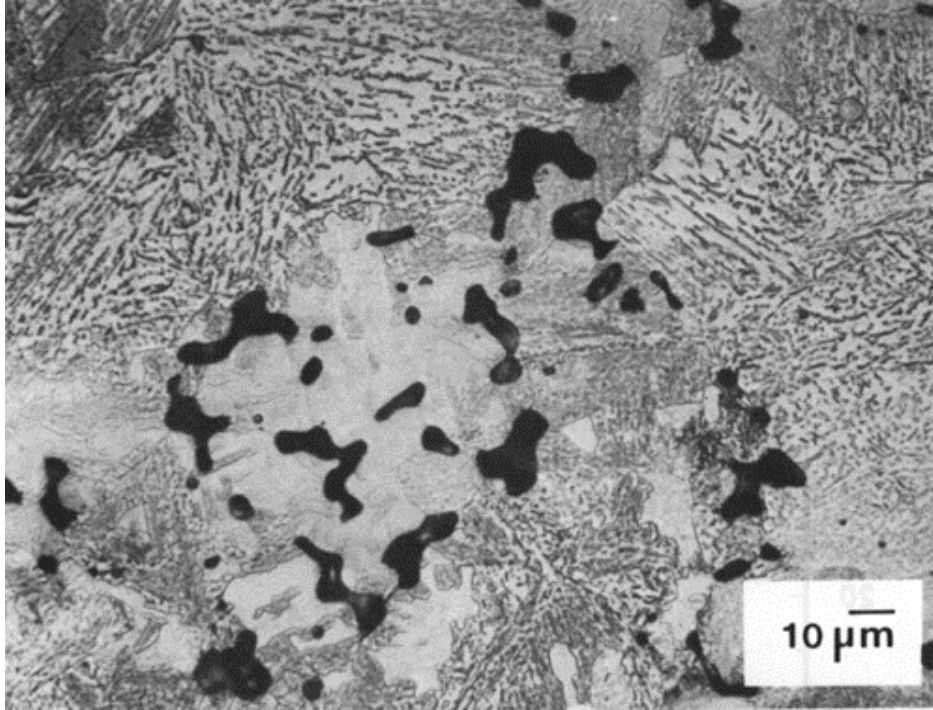
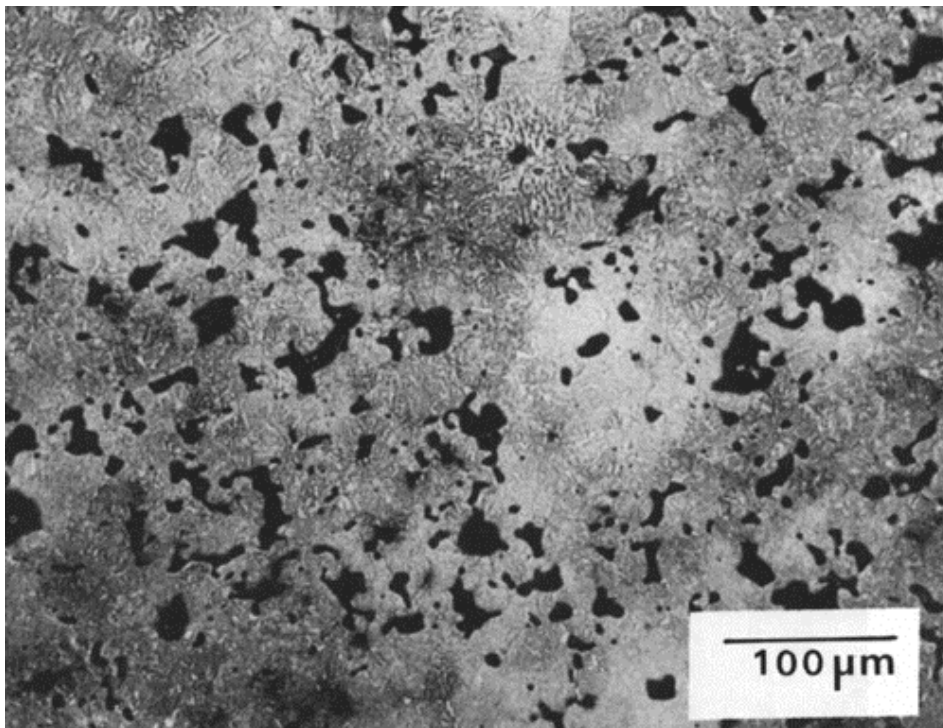


Figure 11: Photomicrographs of the 0.85% Mo prealloy with 0.75% Cr, 0.75% Mn, 1% Ni, and 0.4% graphite - sintered at 2350°F for 30 minutes in D.A. Etched in 2% nital/4% picral.



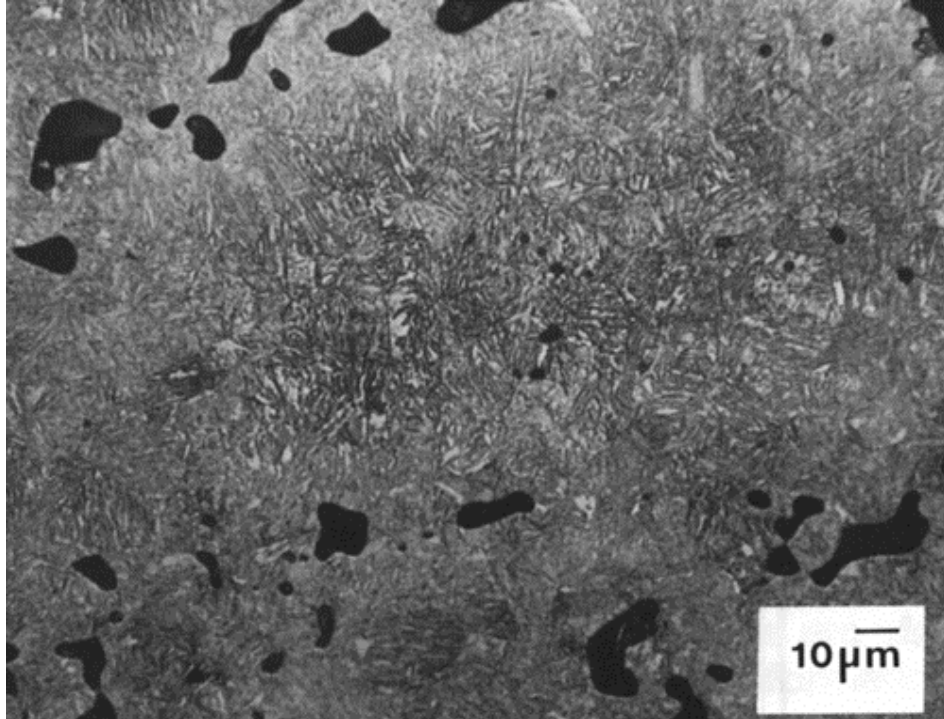


Figure 12: Photomicrographs of the core region of the 0.85% Mo prealloy with 0.75% Cr, 0.75% Mn, 1% Ni, and 0.4% graphite - sintered at 2350°F for 30 minutes in D.A. Quench-hardened and tempered, and plasma nitrided. Etched in 2% nital/4% picral.

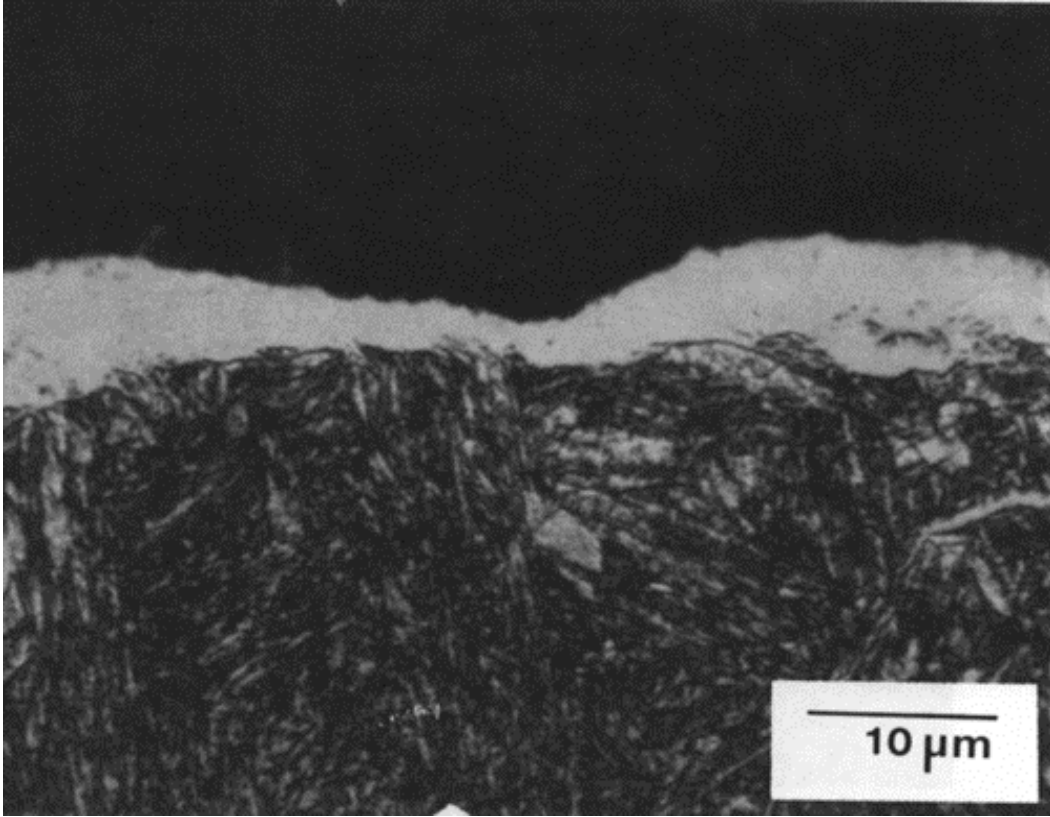


Figure 13: Photomicrograph of the surface of the plasma nitrided sample shown in Figure 12.

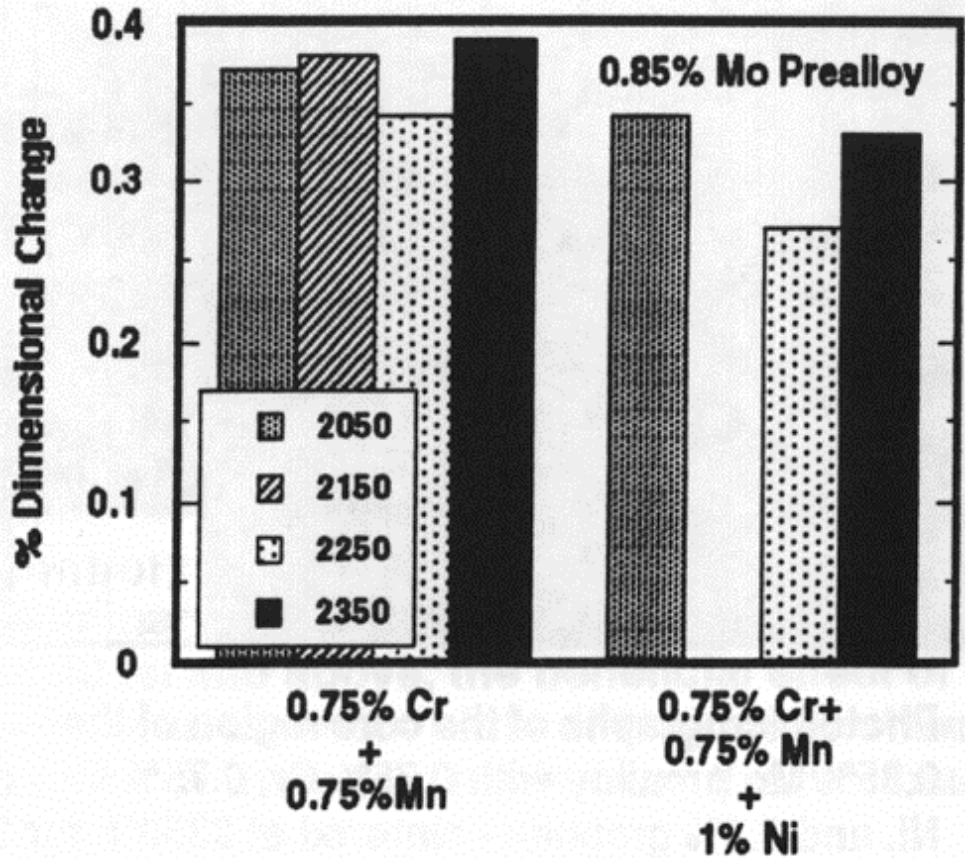


Figure 14: Effect of sintering temperature on dimensional change (45 tsi)



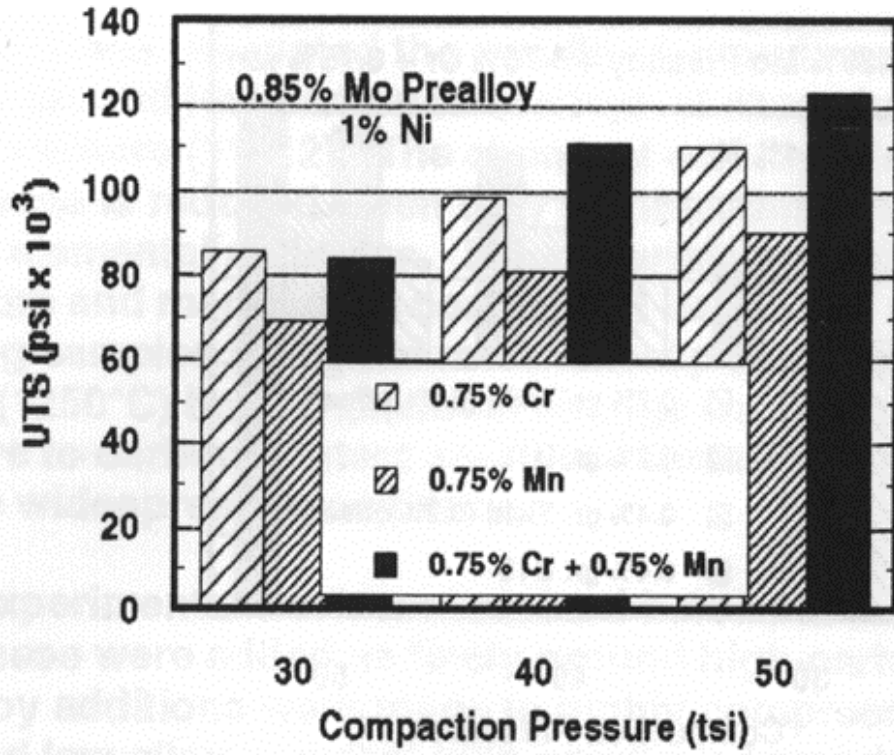


Figure 15: Effect of compaction pressure on UTS. Samples sintered at 2350°F.

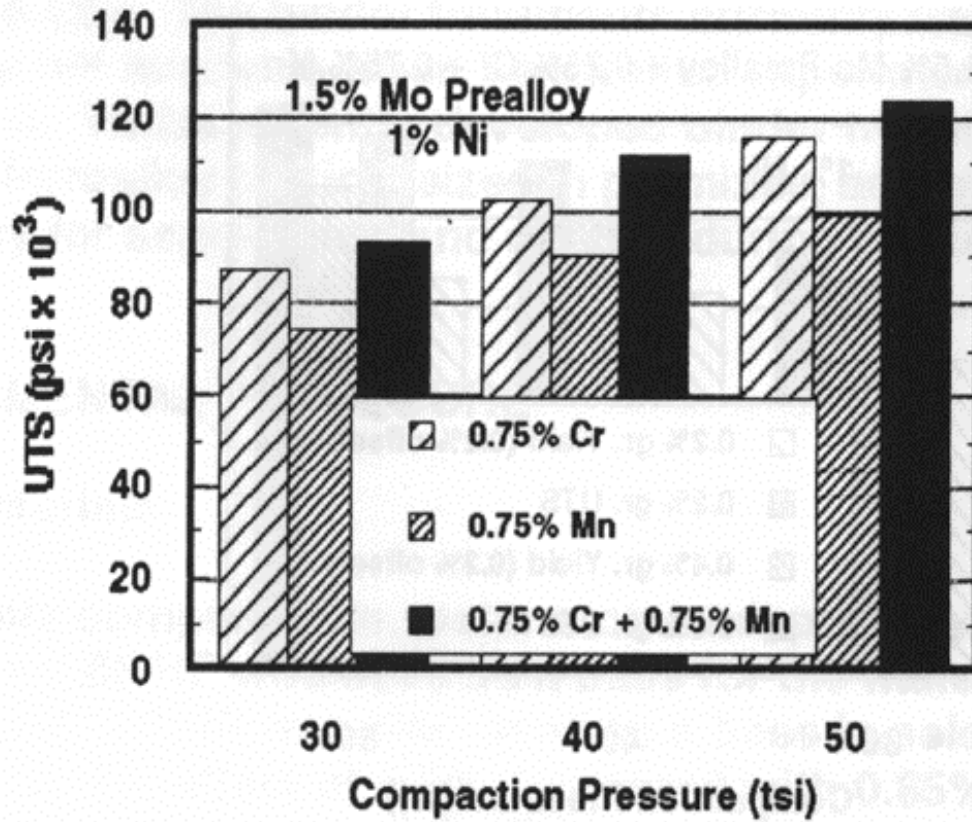


Figure 16: Effect of compaction pressure on UTS. Samples sintered at 2350°F.

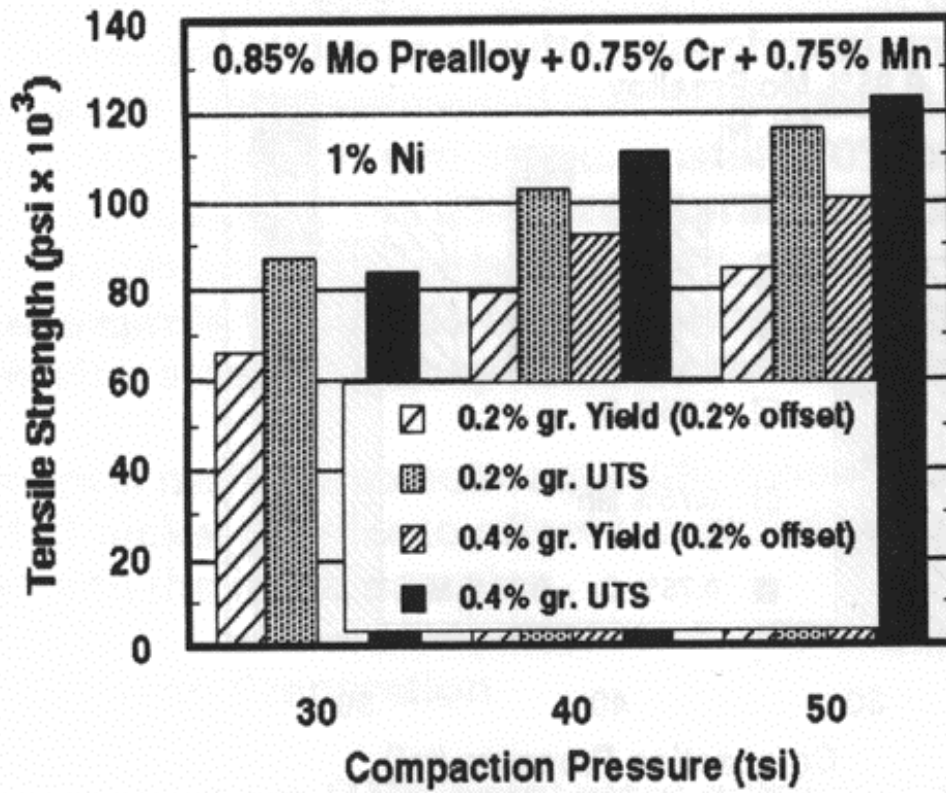


Figure 17: Effect of compaction pressure and graphite addition on tensile strength (2350°F).

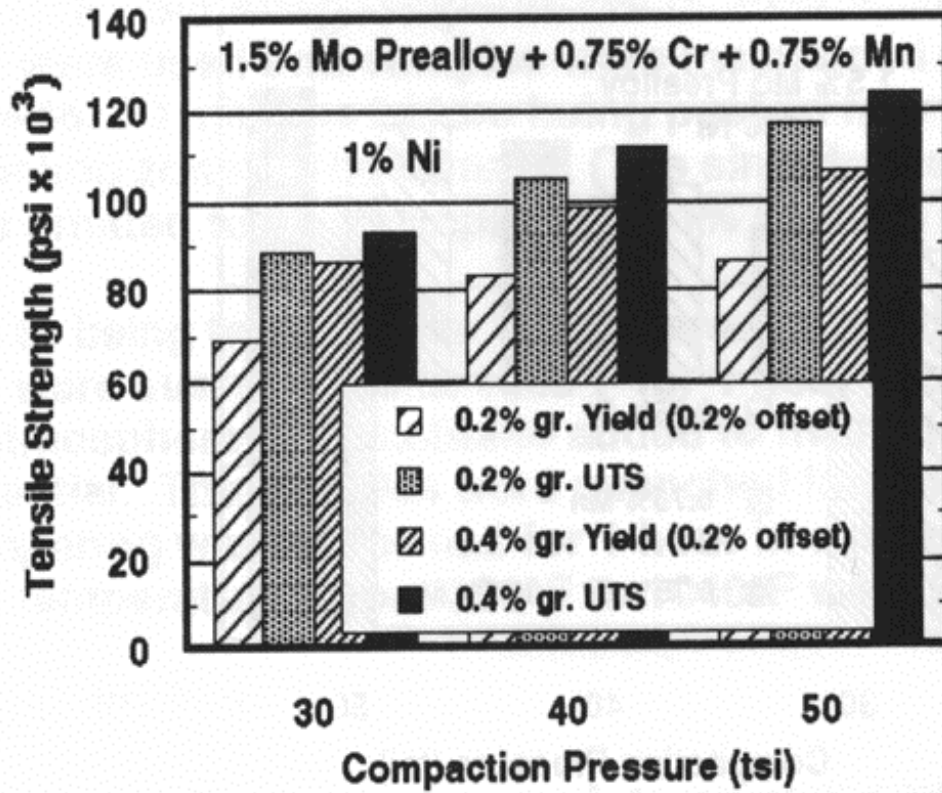


Figure 18: Effect of compaction pressure and graphite addition on tensile strength (2350°F).

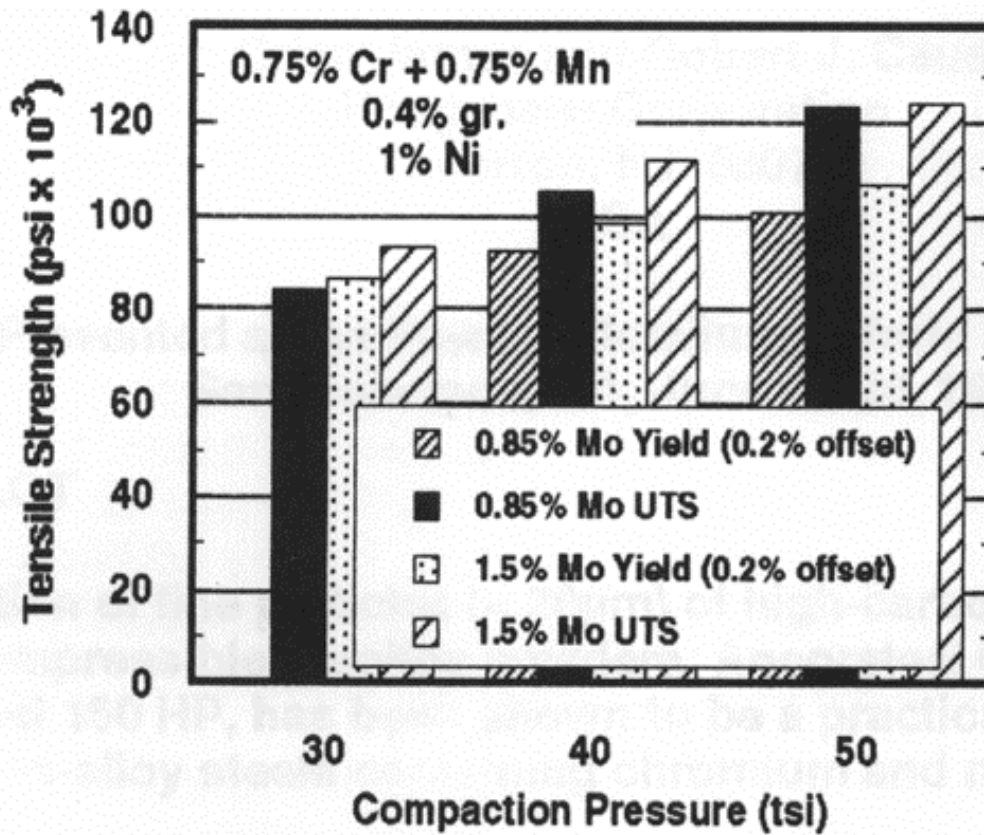


Figure 19: Effect of compaction pressure and base low-alloy powder on tensile strength (2350°F).

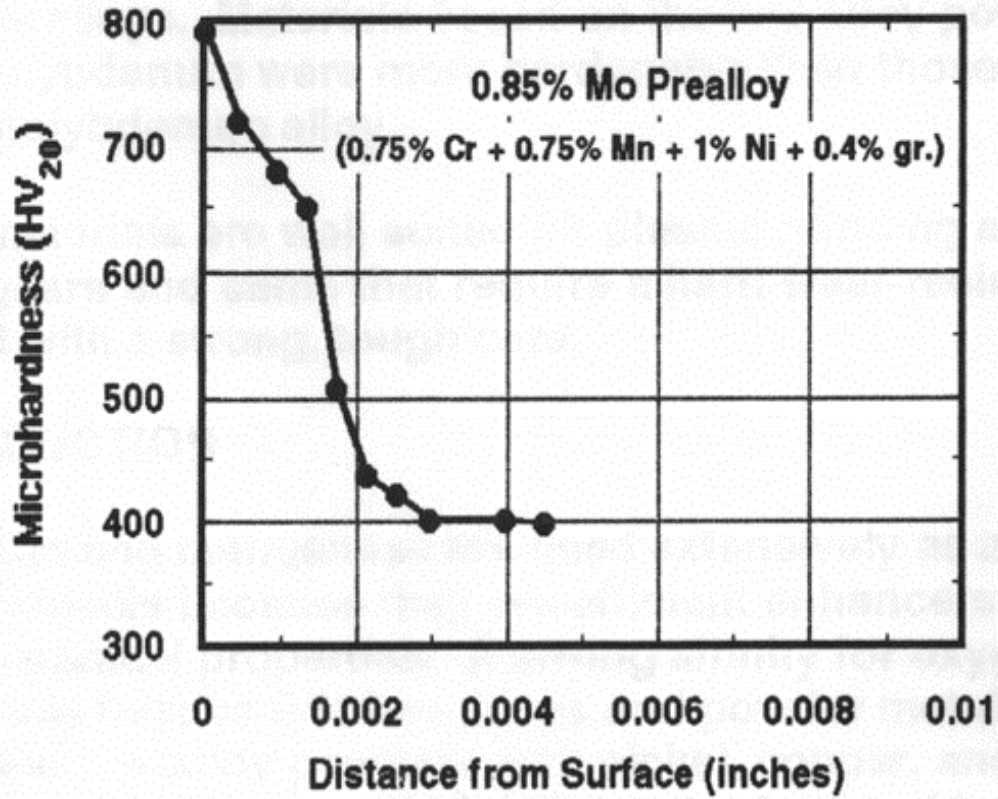


Figure 20: Vickers microhardness profile at the surface of the plasma nitrided sample shown in Figure 13.